Acta Cryst. (1993). A**49**, 722–729

Convergent-Beam Electron Diffraction Study of Incommensurately Modulated Crystals. I. (3+1)-Dimensional Point Groups

BY MASAMI TERAUCHI AND MICHIYOSHI TANAKA

Research Institute for Scientific Measurements, Tohoku University, Sendai 980, *Japan*

(*Received* 15 *December* 1992; *accepted* 6 *April* 1993)

Abstract

The interrelation between the symmetries of convergent-beam electron diffraction (CBED) patterns and the (3+1)-dimensional point groups of one-dimensional incommensurately modulated crystals is discussed. The symmetry subsymbol $\bar{1}$ for the modulated structure implies that the incommensurate reflections show no symmetry in the CBED pattern. The symmetry subsymbols other than $\bar{1}$ imply that the incommensurate reflections exhibit the same symmetries as those of the average structure. These results are demonstrated using the CBED patterns obtained from the one-dimensional incommensurately modulated crystals of $Sr_2Nb_2O_7$ and $Bi_2Sr_2CaCu_2O_{8+\delta}$. It is shown that the CBED method can identify the (3+1)-dimensional point groups of one-dimensional incommensurately modulated structures.

1. Introduction

The method of point-group determination using convergent-beam electron diffraction (CBED) patterns has been established for usual (commensurate) crystals (Goodman, 1975; Buxton, Eades, Steeds & Rackham, 1976; Tanaka, Saito & Sekii, 1983; Tanaka & Terauchi, 1985; Tanaka, 1989). The patterns provide diffracted intensity distribution as a function of the excitation error (rocking curves). Since the CBED method is based upon dynamical diffraction, it can distinguish nonpolar crystals from polar crystals. As a result, the method allows the unique identification of all the point groups. The space-group determination using CBED patterns is based on dynamical extinction (Gjønnes–Moodie lines), which permits an ambiguous identification of 2_1 screw axes and glide planes (Gjønnes & Moodie, 1965). 181 space groups can be uniquely identified using Gjønnes–Moodie lines (Tanaka, Sekii & Nagasawa, 1983; Tanaka, Terauchi & Kaneyama, 1988). The CBED method has been applied successfully to the symmetry determination of many materials (*e.g.* Tanaka, Sekii & Ohi, 1985; Tanaka, 1987; Tanaka, Tsuda *et al.*, 1987).

Furthermore, the CBED method can also reveal the characters of crystal-lattice defects: the shift vectors of stacking faults (Johnson, 1972; Tanaka & Kaneyama, 1986; Tanaka, Yamada & Terauchi, 1992), the Burgers vectors of dislocations (Carpenter & Spence, 1982; Cherns & Preston, 1986; Tanaka *et al.*, 1988), the tilt angles of coherent twin boundaries (Tanaka, Terauchi & Kaneyama, 1991) and the strain distribution near the interfaces of multilayer films (Gat & Schapink, 1987; Cherns, Kiely & Preston, 1988; Humphreys, Eaglesham, Maher & Fraser, 1988).

Recently, attention has been paid to the determination of atom positions (structure analysis) by CBED analysis (Vincent, Bird & Steeds, 1984; Tanaka & Tsuda, 1990, 1991) and to the determination of symmetries of higher-dimensional crystals or incommensurately modulated crystals and quasicrystals (Tanaka, Terauchi, Hiraga & Hirabayashi, 1985; Tanaka, Terauchi, Suzuki, Hiraga & Hirabayashi, 1987; Saito, Tanaka, Tsai, Inoue & Masumoto, 1992). The incommensurately modulated crystals do not have three-dimensional lattice periodicity and are not described by three-dimensional space groups. The crystals, however, recover lattice periodicity in a space higher than three dimensions. de Wolff (1974, 1977) showed that one-dimensional displacively and substitutionally modulated crystals can be described as a three-dimensional section of a (3+1)-dimensional periodic crystal. Janner & Janssen (1980) developed a more general approach to describe the modulated crystals with n modulations as the (3+n)-dimensional periodic crystals (n = 1, 2, ...). Yamamoto (1982) had derived a general structure-factor formula for the n-dimensionally modulated crystal (n = 1, 2, ...), which holds for both displacively and substitutionally modulated crystals. The tables of the (3+1)-dimensional space groups for one-dimensional incommensurately modulated crystals were given by de Wolff, Janssen & Janner (1981). Later, some corrections of the tables were reported by Yamamoto, Janssen, Janner & de Wolff (1985). The analysis of incommensurately modulated crystals using the (3+1)-dimensional space groups has become familiar in the field of X-ray structure analysis.

The CBED method was applied to the study of incommensurately modulated crystals by Steeds *et al.* (1985) and Tanaka *et al.* (1988). However, the (3+1)-dimensional analysis of CBED patterns obtained from incommensurately modulated crystals has never been carried out. The CBED method is expected to be capable of extension in its symmetry determination to higher-dimensional crystals or to the determination of higher-dimensional point groups and space groups. It should

ISSN 0108-7673

be noted that the knowledge of the (3+1)-dimensional space group of a modulated crystal enables us to reduce the number of parameters to be determined in structure analysis. In the present study, we clarify the theory interrelating the symmetries of CBED patterns and (3+1)-dimensional point-group symbols for incommensurately modulated crystals. The theoretical results are verified using the crystals of $Sr_2Nb_2O_7$ and $Bi_2Sr_2CaCu_2O_{8+\delta}$ with incommensurate modulations.

2. Symmetries of CBED patterns obtained from incommensurately modulated crystals

2.1. *Displacively modulated crystals*

Fig.1(*a*) illustrates the (3+1)-dimensional description of a one-dimensional displacively modulated structure. The arrows labeled a_1-a_3 and a_4 indicate the (3+1)-dimensional crystal axes. The horizontal line labeled R_3 represents the three-dimensional space (real world). In the (3+1)-dimensional description, an atom is not located at a point as in three-dimensional space but expressed by a string, which extends along the fourth direction a_4 perpendicular to the three-dimensional space R_3. The parallelogram drawn with thick lines is a unit cell in the (3+1)-dimensional space. The unit cell contains two atom strings. The wavy shape of the atom strings, which are periodic along a_4, represents a displacive-type modulation. The width of the atom strings indicates the spread of the atom in R_3. The atom positions of the modulated structures in R_3 are given as a three-dimensional section of the atom strings in the (3+1)-dimensional space. The diffraction vector $\mathbf{G}$ is written as

$$\mathbf{G} = h_1\mathbf{a}^* + h_2\mathbf{b}^* + h_3\mathbf{c}^* + h_4\mathbf{k},$$

where a set of $h_1h_2h_3h_4$ is a (3+1)-dimensional reflection index and $\mathbf{a}^*, \mathbf{b}^*$ and $\mathbf{c}^*$ are the reciprocal-lattice vectors of the real lattice vectors $\mathbf{a}, \mathbf{b}$ and $\mathbf{c}$ of the average structure. The modulation wave vector $\mathbf{k}$ is written as

$$\mathbf{k} = k_1\mathbf{a}^* + k_2\mathbf{b}^* + k_3\mathbf{c}^*,$$

where one coefficient of k_i (i = 1-3) is an irrational number and the others are rational. The structure factor $F(h_1h_2h_3h_4)$ for the (3+1)-dimensional crystal is given by de Wolff (1974, 1977) as follows:

$$F(h_1h_2h_3h_4) = \sum_{\mu=1}^{N} f_\mu \exp 2\pi i(h_1\overline{x_1^\mu} + h_2\overline{x_2^\mu} + h_3\overline{x_3^\mu}) \times \int_0^1 \exp 2\pi i\left[\sum_{i=1}^{3}(h_i + h_4k_i)u_i^\mu + h_4\overline{x_4^\mu}\right] d\overline{x_4^\mu}, \quad (1)$$

where

$$\overline{x_4^\mu} = (\overline{x_1^\mu} + n_1)k_1 + (\overline{x_2^\mu} + n_2)k_2 + (\overline{x_3^\mu} + n_3)k_3.$$

The symbols f_μ and $\overline{x_i^\mu}$ (i = 1-3) are the atom form factor and the ith component of the position of the μth atom in the unit cell of the average structure, respectively. The symbol u_i^μ is the ith component of the displacement from the atom position $\overline{x_i^\mu}$ of the μth atom. Since the atom in the (3+1)-dimensional space is continuous along a_4 and discrete along R_3, the structure factor is expressed by the summation in R_3 and the integration along a_4. A three-dimensional section of the (3+1)-dimensional unit cell gives a modulated atomic arrangement at a unit cell of the average structure in R_3. Then, the atom strings in the (3+1)-dimensional unit cell correspond to the sum of the atom displacements over an infinite number of the unit cells of the average structure. This means that (1) is the structure factor for the unit cell with lattice parameter of infinite length in R_3 along the direction of the modulation wave vector $\mathbf{k}$.

The CBED patterns are obtained from a finite area of a crystal. Hence, it is necessary to use the structure

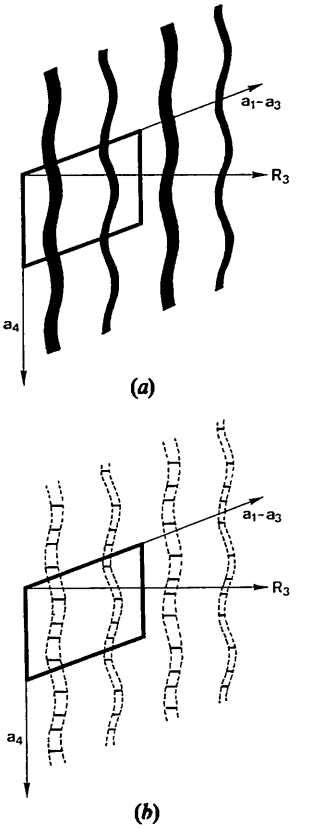

Fig. 1. (*a*) The (3+1)-dimensional description of a one-dimensional displacively modulated structure. The wavy strings are the (3+1)-dimensional description of atoms with a displacive modulation. (*b*) A finite number of the three-dimensional sections of the atom strings in the (3+1)-dimensional unit cell, which corresponds to a finite volume of the modulated structure in R_3.

factor, which takes account of the effect of the finite size, to discuss the symmetries of the CBED patterns obtained from the modulated structures. A finite volume of a modulated structure in R_3 corresponds to a finite number of the three-dimensional sections of the atom strings in the (3+1)-dimensional unit cell as indicated in Fig.1(*b*). The structure factor for the finite volume is derived from (1) by rewriting the integration over a unit length along a_4 with the summation over a finite number of three-dimensional sections of the atom strings. Then, the structure factor for the finite volume $F'(h_1h_2h_3h_4)$ is written as

$$F'(h_1h_2h_3h_4) = \sum_{\mu=1}^{N} f_\mu \exp 2\pi i(h_1\overline{x_1^\mu} + h_2\overline{x_2^\mu} + h_3\overline{x_3^\mu}) \times \left\{ \sum_{n_1}\sum_{n_2}\sum_{n_3} \exp 2\pi i \times \left[\sum_{i=1}^{3} (h_i + h_4k_i)u_i^\mu + h_4\overline{x_4^\mu} \right] \right\}, \quad (2)$$

where $N_1 < n_1 \leq N_1'$, $N_2 < n_2 \leq N_2'$, $N_3 < n_3 \leq N_3'$ and $N' = (N_1' - N_1)(N_2' - N_2)(N_3' - N_3)$ is the number of the unit cells of the average structure included in the specimen volume from which the CBED pattern is taken. The term in { } in (2) expresses the effect of the finite volume on the diffracted intensity.

The symmetries of the CBED patterns can be determined by examination of the symmetries of the structure factor $F'(h_1h_2h_3h_4)$. For simplicity, we assume that the modulation wave vector is written as $\mathbf{k} = k_3\mathbf{c}^*$ and the modulated structure belongs to the (3+1)-dimensional space group $P_{\ 1\ \bar{1}}^{P2/m}$. This space-group symbol indicates: (i) the modulation wave vector $\mathbf{k}$ exists inside the first Brillouin zone for the average structure (P); (ii) the average structure belongs to the space group $P2/m$; (iii) the modulated structure has a twofold rotation axis, which is common to both the average and modulated structures (subsymbol 1) but does not have the mirror symmetry possessed by the average structure (subsymbol $\bar{1}$). For the twofold rotation axis of this (3+1)-dimensional space group, the structure factor $F'(h_1h_2h_3h_4)$ [(2)] is written as

$$F'(h_1h_2h_3h_4) = \sum_{\mu=1}^{N} f_\mu \exp 2\pi i(h_1\overline{x_1^\mu} + h_2\overline{x_2^\mu} + h_3\overline{x_3^\mu}) \times \left\{ \sum_{n_3} \exp 2\pi i[h_1u_1^\mu + h_2u_2^\mu + (h_3 + h_4k_3)u_3^\mu + h_4\overline{x_4^\mu}] \right\} + \sum_{\mu=1}^{N} f_\mu \exp 2\pi i(-h_1\overline{x_1^\mu} - h_2\overline{x_2^\mu} + h_3\overline{x_3^\mu}) \left\{ \sum_{n_3} \exp 2\pi i[-h_1u_1^\mu - h_2u_2^\mu + (h_3 + h_4k_3)u_3^\mu + h_4\overline{x_4^\mu}] \right\}, \quad (3)$$

where $\overline{x_4^\mu} = (\overline{x_3^\mu} + n_3)k_3$. The terms within { } in (3) represent the effect of the finite volume on the diffracted intensity.

We consider the reflections $h_1h_2h_3h_4$ and $\bar{h}_1\bar{h}_2h_3h_4$, which are equivalent with respect to the twofold rotation axis of the average structure. The symmetry subsymbol 1, which is written beneath symmetry symbol 2 in the expression for the (3+1)-dimensional space group, indicates that the modulation wave vector $\mathbf{k}$ is transformed into itself by symmetry operation 2 of the average structure. It is clear from (3) that the structure factor $F'(\bar{h}_1\bar{h}_2h_3h_4)$ is equal to the structure factor $F'(h_1h_2h_3h_4)$. Hence, the intensities of the $h_1h_2h_3h_4$ and $\bar{h}_1\bar{h}_2h_3h_4$ reflections are equal. It is clarified that the symmetry of the reflections ($h_4 \neq 0$) due to the modulated structure (incommensurate reflections) is the same as that of the fundamental reflections ($h_4 = 0$) due to the average structure with respect to the twofold rotation axis of the average structure. Next, we consider the reflections $h_1h_2h_3h_4$ and $h_1h_2\bar{h}_3\bar{h}_4$, which are equivalent with respect to the mirror symmetry of the average structure. The symmetry subsymbol $\bar{1}$, which is written beneath symmetry symbol m in the expression for the (3+1)-dimensional space group, indicates that the modulation wave vector $\mathbf{k}$ is transformed into $-\mathbf{k}$ by the symmetry operation m. For the incommensurate reflections ($h_4 \neq 0$), the corresponding formula to the terms within { } of $F'(h_1h_2h_3h_4)$ in (3) are not equal to those of $F'(h_1h_2\bar{h}_3\bar{h}_4)$ because k_3 is an irrational number. Hence, the intensity of the $h_1h_2h_3h_4$ reflection is not equal to that of the $h_1h_2\bar{h}_3\bar{h}_4$ reflection. For the fundamental reflections ($h_4 = 0$), the intensity of the $h_1h_2h_30$ reflection is equal to that of the $h_1h_2\bar{h}_30$ reflection because $F'(h_1h_2h_30)$ is equal to $F'(h_1h_2\bar{h}_30)$. It should be noted that this mirror symmetry m between the fundamental reflections is expected to be destroyed owing to the dynamical diffraction effect between the fundamental and incommensurate reflections. In most modulated structures, however, the amplitude of the modulation wave u_i^μ is not so large as to affect the symmetry of the fundamental reflections. Therefore, the fundamental reflections should show the symmetry of the average structure, while the incommensurate reflections lose this symmetry. The results obtained are summarized by the following rules.

1. For symmetry symbol 1, both the fundamental and incommensurate reflections show the symmetries of the average structure.

2. For symmetry symbol $\bar{1}$, the fundamental reflections, in practice, show the symmetries of the average

structure but the incommensurate reflections do not have any symmetries.

Rule 1 also holds for the symmetry symbols *s*, *t*, *q* and *h* of the (3+1)-dimensional space groups because those space-group symbols are expressed by symbol 1 in the frame of the (3+1)-dimensional point groups.

Equations (2) and (3) hold for any numbers N', N_i and N_i' (i = 1-3). A change of N_i and N_i' (i = 1-3) with N' kept constant corresponds to a change of the illuminated specimen position, from which the CBED pattern is taken, without changing the illuminated volume. A change of all the numbers N', N_i and N_i' (i = 1-3) corresponds to a change in both the illuminated volume and the specimen position. With these changes, the magnitude of the structure factor changes but the symmetry of the structure factor is unchanged. Even if N' is reduced to one, (2) and (3) still hold. This indicates that the symmetry of the incommensurately modulated structure should appear in principle even in a CBED pattern taken from one unit cell of the average structure. These facts lead to the following results.

(*a*) Even if the size and the position of an illuminated specimen area are changed, the intensity distribution in the CBED pattern changes but the symmetry of the pattern does not change.

(*b*) The (3+1)-dimensional symmetries can appear in CBED patterns if more than one unit cell of the average structure are included in the volume from which the CBED pattern is obtained. In other words, to obtain the symmetries expected from the (3+1)-dimensional symmetry symbols, it is not necessary to take the CBED pattern from such a large specimen area whose diameter is larger than the approximate period of the modulated structure (the approximate least common multiple between the modulation wavelength and the unit-cell length of the average structure).

These results as a whole ensure that the (3+1)-dimensional symmetries appear in the CBED patterns taken from a finite volume of the incommensurately modulated crystals.

We have described how the (3+1)-dimensional point groups can be determined by the examination of CBED symmetries of fundamental and incommensurate reflections using rules 1 and 2. However, it is worthwhile to note the following facts. If the point-group symmetry of the average structure and the modulation wave vector **k** are completely known, the (3+1)-dimensional point groups themselves are determined by inspecting only how the modulation wave vector **k** is transformed by the symmetry operations of the average structure, although the symmetries of incommensurate reflections provide important information for the confirmation of the point groups. From this, it is seen that the correct determination of the point-group symmetry of the average structure is very important in the determination of the (3+1)-dimensional point groups. Then, there is no doubt that the point groups of the average structure can be determined unambiguously by the CBED method when the amplitude of the modulation wave u_i^μ is not so large as to affect the symmetry of the fundamental reflections.

It should be noted that the structure analysis of incommensurately modulated crystals with CBED is difficult for the following reason. Since the experimental intensities of CBED patterns are obtained from a finite volume of incommensurately modulated crystals, (2) has to be applied instead of (1). However, there is no way to determine from experiment the correct volume to be summed in (2). In this case, we cannot reproduce the observed intensities using (2). Real X-ray structure analysis of the modulated crystals, in which the illuminated volume is much larger than that in CBED, may be conducted using (1) since the volume may be regarded as infinitely large.

2.2. *Substitutionally modulated crystals*

The substitutional modulation arises from a periodic variation of the site occupation probability of atoms. This type of modulated structure is also described by the (3+1)-dimensional periodic structure. This type of modulation does not originate from the modulation of the atomic displacement u_i^μ with x_4 as in the case of the displacive type, but is expressed by the modulation of the atom form factor f_μ in (1) with x_4. By substituting zero for the displacements of atoms u_i^μ in (1), the structure factor for this type of modulated structure is written as follows (de Wolff, 1974, 1977):

$$F(h_1h_2h_3h_4) = \sum_{\mu=1}^{N} \exp 2\pi i(h_1x_1^\mu + h_2x_2^\mu + h_3x_3^\mu) \times \int_0^1 f_\mu(x_4^\mu) \exp(2\pi i h_4 x_4^\mu) \mathrm{d}x_4^\mu, \quad (4)$$

where $x_4^\mu = (x_1^\mu + n_1)k_1 + (x_2^\mu + n_2)k_2 + (x_3^\mu + n_3)k_3$. The integration over a unit length along a_4 indicates that the structure factor stands for the unit cell with the lattice parameter of an infinite length along the direction of the modulation wave vector **k**. The structure factor for a finite specimen volume $F'(h_1h_2h_3h_4)$ is written as

$$F'(h_1h_2h_3h_4) = \sum_{\mu=1}^{N} \exp 2\pi i(h_1x_1^\mu + h_2x_2^\mu + h_3x_3^\mu) \times \left\{ \sum_{n_1}\sum_{n_2}\sum_{n_3} f_\mu(x_4^\mu) \exp(2\pi i h_4 x_4^\mu) \right\}, \quad (5)$$

where $N_1 < n_1 \leq N_1'$, $N_2 < n_2 \leq N_2'$, $N_3 < n_3 \leq N_3'$ and $N' = (N_1' - N_1)(N_2' - N_2)(N_3' - N_3)$ is the number of unit cells of the average structure included in the specimen volume. The term in { } in (5) expresses the effect of the finite volume. For simplicity, we again assume that the modulation wave vector is written as

$\mathbf{k} = k_3\mathbf{c}^*$ and the modulated structure belongs to the (3+1)-dimensional space group $P^{P2/m}_{1\ \bar{1}}$ like the case in § 2.1. For the twofold rotation axis of this space group, the structure factor of (5) is written as

$$F'(h_1h_2h_3h_4) = \sum_{\mu=1}^{N} \exp 2\pi i(h_1x_1^\mu + h_2x_2^\mu + h_3x_3^\mu) \times \left\{\sum_{n_3} f_\mu(x_4^\mu) \exp(2\pi i h_4 x_4^\mu)\right\} + \sum_{\mu=1}^{N} \exp 2\pi i(-h_1x_1^\mu - h_2x_2^\mu + h_3x_3^\mu) \times \left\{\sum_{n_3} f_\mu(x_4^\mu) \exp(2\pi i h_4 x_4^\mu)\right\}, \quad (6)$$

where $x_4^\mu = (x_3^\mu + n_3)k_3$. The terms within { } in (6) express the effect of the finite volume.

For the $h_1h_2h_3h_4$ and $\bar{h}_1\bar{h}_2h_3h_4$ reflections, which are equivalent with respect to the twofold rotation axis of the average structure, the structure factors $F'(\bar{h}_1\bar{h}_2h_3h_4)$ and $F'(h_1h_2h_3h_4)$ are the same, indicating that the intensities of these reflections are equal. Hence, the symmetry of the incommensurate reflections ($h_4 \neq 0$) is the same as that of the fundamental reflections ($h_4 = 0$) with respect to the twofold rotation axis of the average structure. For the $h_1h_2h_3h_4$ and $h_1h_2\bar{h}_3\bar{h}_4$ reflections, which are equivalent with respect to the mirror symmetry of the average structure, the intensity of the $h_1h_2h_3h_4$ reflection ($h_4 \neq 0$) is not equal to that of the $h_1h_2\bar{h}_3\bar{h}_4$ reflection because the corresponding formula to the terms within { } of $F'(h_1h_2h_3h_4)$ in (6) are not equal to those of $F'(h_1h_2\bar{h}_3\bar{h}_4)$. From the repetition of a similar argument described in a previous section, the fundamental reflections should exhibit the mirror symmetry but incommensurate reflections lose that symmetry. Therefore, rules 1 and 2 given in § 2.1 also hold for the substitutionally modulated crystals.

In the substitutionally modulated case, the atom form factor f_μ cannot be determined by one unit cell of the average structure but is determined by the average over a large number of unit cells. Thus, the symmetries of this type of modulated structure are not determined from one unit cell of the average structure, as in the case of the displacively modulated structure. Since the CBED patterns, however, are taken usually from a specimen volume of ~10 nm diameter × ~100 nm thickness, the volume is large enough to obtain the average value of the occupation or the average atom form factor. Therefore, the CBED patterns taken with usual conditions also exhibit the (3+1)-dimensional symmetries for the substitutionally modulated crystals.

3. Experimental results

3.1. *Experimental results*

The following experiments have been carried out with an electron probe size of ~3 nm diameter. It should be noted that the probe size is smaller than the approximate period of the modulated structure, ~40 nm for $Sr_2Nb_2O_7$ and ~12 nm for $Bi_2Sr_2CaCu_2O_{8+\delta}$.

3.1.1. $Sr_2Nb_2O_7$. Many materials of the $A_2B_2O_7$ family undergo phase transformations from the space group $Cmcm$ to $Cmc2_1$ and further to $P2_1$ with decreasing temperature. An incommensurate phase appears, for example, between the phase with $Cmc2_1$ and that with $P2_1$ in $La_2Ti_2O_7$ (Tanaka, Sekii & Ohi, 1985). $Sr_2Nb_2O_7$ transforms from the phase with $Cmc2_1$ into the incommensurate phase at 488 K with a modulation wave vector of $\mathbf{k} = (\frac{1}{2} - \delta)\mathbf{a}^*$ ($\delta = 0.009$-0.023) but does not transform into the phase with $P2_1$. The symmetry of the incommensurately modulated structure of $Sr_2Nb_2O_7$ is expressed by the (3+1)-dimensional space group $P^{Cmc2_1}_{\bar{1}\,s\bar{1}}$ (Yamamoto, 1988).† Then, the (3+1)-dimensional point group of the structure is written as $\frac{mm2}{\bar{1}\,1\,\bar{1}}$. The symbol implies the following substance. The modulation wave vector $\mathbf{k}$ is transformed to $-\mathbf{k}$ by a mirror symmetry operation perpendicular to the a axis $(\frac{m}{\bar{1}})$ and by the twofold rotation-symmetry operation along the c axis $(\frac{2}{1})$. The wave vector is transformed into itself by the mirror symmetry perpendicular to the b axis $(\frac{m}{1})$.

Fig. 2 shows a CBED pattern of the incommensurate phase of $Sr_2Nb_2O_7$ obtained with [010] incidence at an accelerating voltage of 60 kV. The reflections indicated by arrows are incommensurate reflections due to the modulation. Other reflections are fundamental reflections due to the average structure. The (3+1)-dimensional point-group symmetries $(\frac{m}{\bar{1}})$ about the a axis and $(\frac{2}{1})$ about the c axis appear in this CBED pattern. When rule 2 in § 2.1 is considered, symmetry $(\frac{m}{\bar{1}})$ exhibits mirror symmetry perpendicular to the a axis between the fundamental reflections but no mirror symmetry between the incommensurate reflections. The same symmetries are expected from symmetry $(\frac{2}{1})$ in the framework of the projected potential approximation. Fig. 2 shows these symmetries exactly.

Fig. 3 shows a CBED pattern of the incommensurate phase obtained with [201] incidence at an accelerating voltage of 60 kV. The reflections in two rows indicated by arrows are the incommensurate reflections. The other reflections are fundamental ones. The (3+1)-dimensional point-group symmetry about the b axis $(\frac{m}{1})$ appears in

† In the tables of de Wolff *et al.* (1981), the direction of the incommensurate component of the modulation wave vector is taken as the c axis. In the present case, the direction is along the a axis because of the use of the space-group symbol for the average structure normally used. So the expression for the (3+1)-dimensional space group is apparently different from that given in the literature. A similar situation also occurs in the case of $Bi_2Sr_2CaCu_2O_{8+\delta}$.

this pattern. From rule 1 in § 2.1, symmetry $\binom{m}{1}$ displays mirror symmetry perpendicular to the b axis not only between the fundamental reflections but also between the incommensurate reflections. Fig. 3 clearly shows the mirror symmetry between both kinds of reflections. Fig. 4 shows a CBED pattern obtained at the same incidence as in Fig. 3 but from a different specimen area with nearly the same specimen thickness. The pattern shows the same symmetry as in Fig. 3 but the intensity distribution is different. This confirms result (*a*) described in § 2.

3.1.2. $Bi_2Sr_2CaCu_2O_{8+\delta}$. The oxide superconductor $Bi_2Sr_2CaCu_2O_{8+\delta}$ has an incommensurately modulated structure with a modulation wave vector $\mathbf{k} = k_2\mathbf{b}^* + \mathbf{c}^*$ ($k_2 \simeq 1/4.7$). The symmetry of the incommensurate structure of this material is expressed either by a (3+1)-dimensional space group $N\,{}^{Bbmb}_{1\bar{1}1}$ or $N\,{}^{Bb2b}_{111}$ (Yamamoto, Hirotsu, Nakamura & Nagakura, 1989). The symbol N of the space groups indicate the lattice type whose modulation wave vector has the commensurate component $\mathbf{c}^*$. Then, the (3+1)-dimensional point group of the structure is written as ${}^{mmm}_{1\bar{1}1}$ or ${}^{m2m}_{111}$. The two possible (3+1)-dimensional point groups originate from an ambiguous determination of the space group of the average structure.

Fig. 5 shows a CBED pattern of $Bi_2Sr_2CaCu_2O_{8+\delta}$ obtained with [001] incidence at an accelerating voltage of 60 kV. A large size of diffraction discs was chosen for ease of identification of the symmetry of fundamental reflections, where the fundamental and incommensurate reflection discs overlap. The intense diffraction discs are fundamental reflections. The intensities of incommensurate reflection discs are sufficiently weak not to affect the symmetry of fundamental reflections. The fundamental reflections show mirror symmetry perpendicular to the a axis, but do not show mirror symmetry perpendicular to the b axis. These symmetries revealed that the space group of the average structure is not $Bbmb$ but $Bb2b$. Thus, the (3+1)-dimensional point and space groups are determined automatically as ${}^{m2m}_{111}$ and $N\,{}^{Bb2b}_{111}$, respectively, under the modulation wave vector $\mathbf{k} = k_2\mathbf{b}^* + \mathbf{c}^*$.

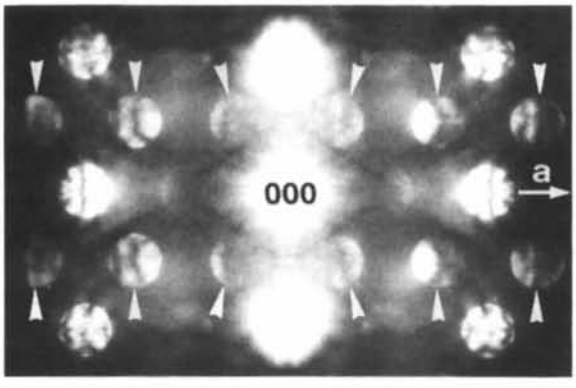

Fig. 2. Convergent-beam electron diffraction (CBED) pattern of the incommensurate phase of $Sr_2Nb_2O_7$ taken with [010] incidence at an accelerating voltage of 60 kV. The reflections indicated by arrows are incommensurate reflections due to the displacive modulation. Other reflections are fundamental reflections due to the average structure. The fundamental reflections show mirror symmetry perpendicular to the a axis, but the incommensurate reflections show no mirror symmetry.

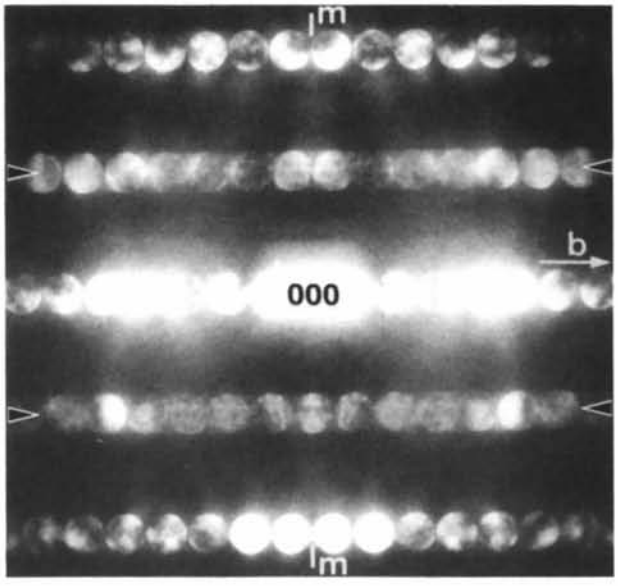

Fig. 3. Convergent-beam electron diffraction (CBED) pattern of the incommensurate phase of $Sr_2Nb_2O_7$ taken with [201] incidence at an accelerating voltage of 60 kV. The reflections at two levels indicated by arrows are the incommensurate ones. Others are fundamental reflections. Both the fundamental and incommensurate reflections show mirror symmetry perpendicular to the b axis.

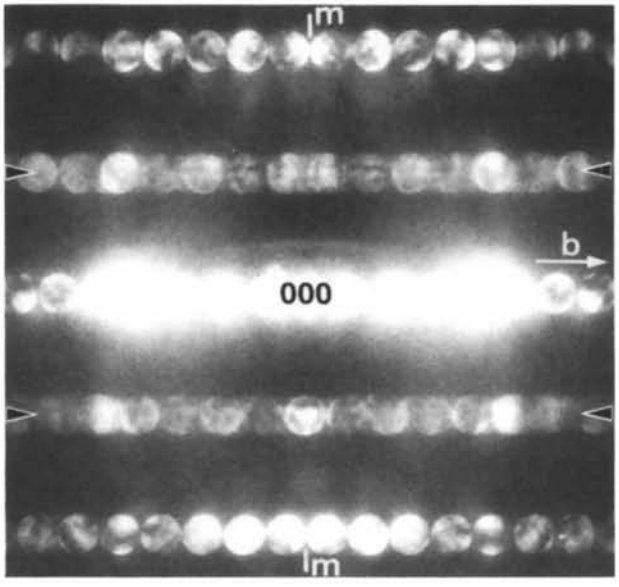

Fig. 4. Convergent-beam electron diffraction (CBED) pattern taken from the incommensurate phase of $Sr_2Nb_2O_7$ with the same incidence as in Fig. 3 but from a different specimen area. The pattern shows the same symmetry as in Fig. 3 but the intensity distribution is different.

Fig. 6 shows a CBED pattern obtained with the same electron incidence as that in Fig. 5 but with the disc size set smaller than that of Fig. 5 to identify the symmetry of the incommensurate reflections, several of them being indicated by arrows. These reflections show mirror symmetry perpendicular to the a axis but do not show mirror symmetry perpendicular to the b axis, as with the fundamental reflections. The symmetry of the incommensurate reflections is confirmed to agree with those expected from (3+1)-dimensional point-group symmetries about the a axis $\left(\begin{smallmatrix} m \\ 1 \end{smallmatrix}\right)$ and the b axis $\left(\begin{smallmatrix} 2 \\ 1 \end{smallmatrix}\right)$ (rule 1). Therefore, these symmetries confirm that the material belongs to the (3+1)-dimensional space group $N\,{}^{Bb2b}_{111}$.

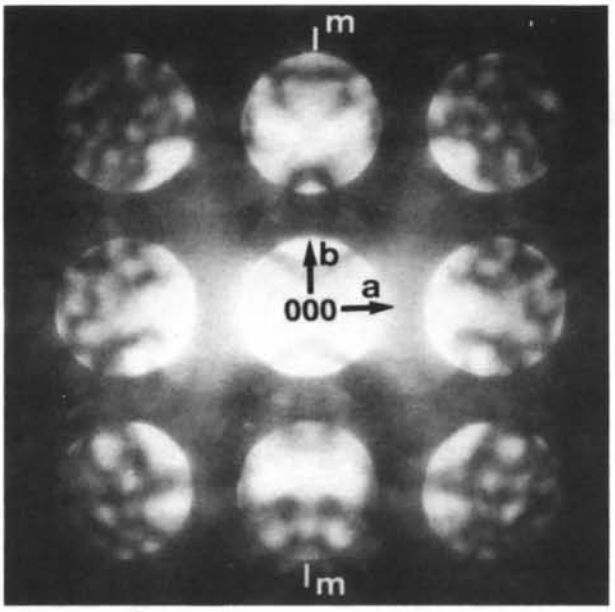

Fig. 5. Convergent-beam electron diffraction (CBED) pattern of $Bi_2Sr_2CaCu_2O_{8+\delta}$ obtained with [001] incidence at an accelerating voltage of 60 kV. The intense diffraction discs are fundamental reflections. These reflections show mirror symmetry perpendicular to the a axis but do not show mirror symmetry perpendicular to the b axis.

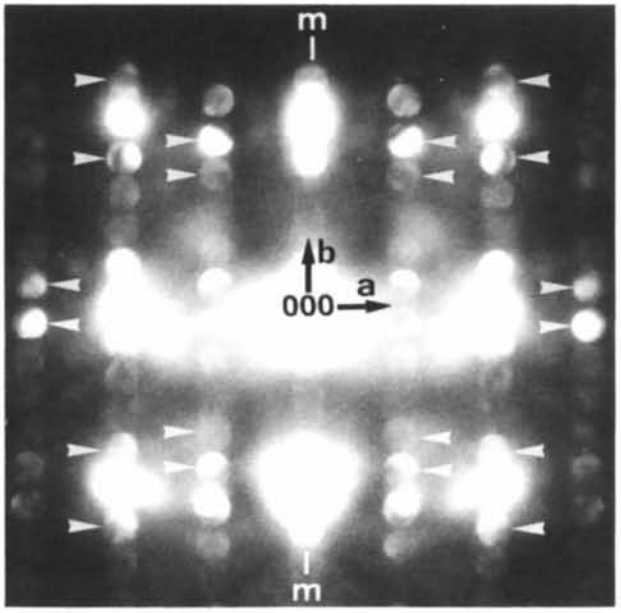

Fig. 6. Convergent-beam electron diffraction (CBED) pattern of $Bi_2Sr_2CaCu_2O_{8+\delta}$ obtained with the same incidence as that in Fig. 5, but the disc size is smaller. The incommensurate reflections, several of them being indicated by arrows, show mirror symmetry perpendicular to the a axis like the fundamental reflections.

The authors thank Dr A.Yamamoto of the National Institute for Research in Inorganic Materials for useful discussions. The present work was supported partly by a Grant-in-Aid for Scientific Research from the Ministry of Education, Science and Culture, Japan.

References

BUXTON, B. F., EADES, J., STEEDS, J. W. & RACKHAM, G. M. (1976). *Philos. Trans. R. Soc. London*, **281**, 171-194.

CARPENTER, R. W. & SPENCE, J. C. H. (1982). *Acta Cryst.* A**38**, 55-61.

CHERNS, D., KIELY, C. J. & PRESTON, A. R. (1988). *Ultramicroscopy*, **24**, 355-370.

CHERNS, D. & PRESTON, A. R. (1986). Proc. XIth International Congress on Electron Microscopy, Kyoto, Japan, pp. 721-722.

GAT, R. & SCHAPINK, F. W. (1987). *Ultramicroscopy*, **21**, 389-392.

GJØNNES, J. & MOODIE, A. F. (1965). *Acta Cryst.* **19**, 65-67.

GOODMAN, P. (1975). *Acta Cryst.* A**31**, 804-810.

HUMPHREYS, C. J., EAGLESHAM, D. J., MAHER, D. M. & FRASER, H. L. (1988). *Ultramicroscopy*, **26**, 13-24.

JANNER, A. & JANSSEN, T. (1980). *Acta Cryst.* A**36**, 399-408, 408-415.

JOHNSON, A. W. S. (1972). *Acta Cryst.* A**28**, 89-91.

SAITO, M., TANAKA, M., TSAI, A. P., INOUE, A. & MASUMOTO, T. (1992). *Jpn. J. Appl. Phys.* **31**, L109-L112.

STEEDS, J. W., BIRD, D. M., EAGLESHAM, D. J., MCKERNAN, S., VINCENT, R. & WITHERS, R. L. (1985). *Ultramicroscopy*, **18**, 97-110.

TANAKA, M. (1987). Proc. 45th Annual Meeting of Electron Microscopy Society of America, Baltimore, USA, pp. 20-23.

TANAKA, M. (1989). *J. Electron Microsc. Tech.* **13**, 27-39.

TANAKA, M. & KANEYAMA, T. (1986). Proc. XIth International Congress on Electron Microscopy, Kyoto, Japan, pp. 203-206.

TANAKA, M., SAITO, R. & SEKII, H. (1983). *Acta Cryst.* A**39**, 357-368.

TANAKA, M., SEKII, H. & NAGASAWA, T. (1983). *Acta Cryst.* A**39**, 825-837.

TANAKA, M., SEKII, H. & OHI, K. (1985). *Jpn. J. Appl. Phys.* **24**, Suppl. pp. 814-816.

TANAKA, M. & TERAUCHI, M. (1985). *Convergent-Beam Electron Diffraction*. Tokyo: JEOL-Maruzen.

TANAKA, M., TERAUCHI, M., HIRAGA, K. & HIRABAYASHI, M. (1985). *Ultramicroscopy*, **17**, 279-286.

TANAKA, M., TERAUCHI, M. & KANEYAMA, T. (1988). *Convergent-Beam Electron Diffraction* II. Tokyo: JEOL-Maruzen.

TANAKA, M., TERAUCHI, M. & KANEYAMA, T. (1991). *J. Electron Microsc.* **40**, 211-220.

TANAKA, M., TERAUCHI, M., SUZUKI, S., HIRAGA, K. & HIRABAYASHI, M. (1987). *Acta Cryst.* B**43**, 494-501.

TANAKA, M. & TSUDA, K. (1990). Proc. XIIth International Congress on Electron Microscopy, Seattle, USA, pp. 518-519.

TANAKA, M. & TSUDA, K. (1991). Proc. 26th Meeting of Microbeam Analysis Soc., San Jose, USA, pp. 145-146.

TANAKA, M., TSUDA, K., YAMADA, K., ENDOH, Y., HIDAKA, Y., ODA, M., SUZUKI, T. & MURAKAMI, T. (1987). *Jpn. J. Appl. Phys.* **26**, L1502-L1504.

TANAKA, M., YAMADA, S . & TERAUCHI, M. (1992). Proc. 5th Asia-Pacific Electron Microscopy Conference, Beijing, China, pp. 154-157.

VINCENT, R., BIRD, D. M. & STEEDS, J. W. (1984). *Philos. Mag.* A**50**, 745-763, 765-786.

WOLFF, P. M. DE (1974). *Acta Cryst.* A**30**, 777-785.
WOLFF, P. M. DE (1977). *Acta Cryst.* A**33**, 493-497.
WOLFF, P. M. DE, JANSSEN, T. & JANNER, A. (1981). *Acta Cryst.* A**37**, 625-636.
YAMAMOTO, A. (1982). *Acta Cryst.* A**38**, 87-92.
YAMAMOTO, A., JANSSEN, T., JANNER, A. & DE WOLFF, P. M. (1985). *Acta Cryst.* A**41**, 528-530.
YAMAMOTO, N. (1988). *Solid State Phys.* **23**, 547-556.
YAMAMOTO, N., HIROTSU, Y., NAKAMURA, Y. & NAGAKURA, S. (1989). *Jpn. J. Appl. Phys.* **28**, L598-L601.

Acta Cryst. (1993). A**49**, 729–735

2D Rotation–Translation Coupling with Planar Molecules

BY W. PRESS, C. NÖLDEKE AND A. SCHRÖDER-HEBER
Institut für Experimentalphysik, Universität Kiel, 2300 *Kiel* 1, *Germany*

AND W. PRANDL AND P. SCHIEBEL
Institut für Kristallographie, Universität Tübingen, 7400 *Tübingen, Germany*

(*Received* 24 *December* 1992; *accepted* 16 *April* 1993)

Abstract

A structure-factor calculation for 2D rotation–translation coupling with planar molecules is presented. The starting point is a continuous description of the scattering-length-density distribution for a planar molecule that rotates around its symmetry axis. For the example of a molecule with threefold symmetry at a site with fourfold symmetry, the successive correction terms to the conventional rotational form factor are evaluated. This approach yields results equivalent to the split-molecule model. This is shown by an example of a structure refinement on $Ni(ND_3)_6Br_2$ single-crystal data.

1. Introduction

The description of the thermal motion in the structure analysis of more complex molecular solids continues to be a difficult problem. Particularly in the presence of orientational disorder, powder samples give rise to only a few Bragg peaks of notable intensity, while there may be many model parameters. For atoms (ions), a rather detailed description of the probability density functions (p.d.f.) beyond harmonic motions or the corresponding structure factors are available [cumulant expansion, Gram–Charlier expansion (*International Tables for X-ray Crystallography*, 1974)]. Frequently, disorder aspects are described by split-atom models. For (rigid) molecules or molecular groups, the above approaches can be used for describing the centre-of-mass (c.o.m.) positions of the molecules. Additionally, rotational motions and, possibly, orientational disorder have to be introduced. Again this can be done either with continuous or with discrete models. In the first case, the density distribution on a spherical surface (2D: circle) is expanded into symmetry-adapted surface harmonics (2D: trigonometric functions). In the second case, an appropriate set of discrete molecular orientations is chosen.

Apparently, there are cases where c.o.m. motions and rotational motions do not occur independently and there is a pronounced rotation–translation coupling (RT coupling). A three-dimensional example, CBr_4-I, was described quite a while ago (Press, Grimm & Hüller, 1979; Hohlwein, 1984).

(i) In the first case, a p.d.f., containing both a positional (c.o.m.) and an angular variable, is expanded (Taylor expansion) into symmetry-allowed terms and powers of displacement variables and derivatives of the p.d.f. are combined to give products that are totally symmetric with respect to the symmetry operations of the site symmetry. One may note a simple meaning of RT coupling: the orientational distribution depends on the c.o.m. position, which means that it is different for the equilibrium or displaced c.o.m. position. This is most pronounced for asymmetric molecules (like triangular groups *etc.*) at a site with a centre of symmetry.

(ii) An equivalent access is the 'split-molecule' approach, which can be introduced in two successive steps. C.o.m. displacements lead to low-symmetry sites with a preference for certain orientations. The first approach consists in taking a discrete distribution of the c.o.m.'s over all symmetrically equivalent sites of a lattice position in combination with continuous orientational distributions. It is not particularly useful for practical purposes, but demonstrates the meaning of the model parameters of (i) more explicitly. The most general split-molecule approach uses one or several discrete c.o.m. positions and a set of discrete orientations. A p.d.f. conforming with the